Hydrophobicity and Sliding Behavior of Liquid Droplets on the Fluorinated Latex Films

Jong-Wook Ha,* In Jun Park, and Soo-Bok Lee

Interface Materials and Engineering Laboratory, Korea Research Institute of Chemical Technology, Jang-dong 100, Yuseong, Daejeon 305-343, Korea

Received June 8, 2004; Revised Manuscript Received November 13, 2004

ABSTRACT: The surface properties of latex films prepared from heptadecafluorodecyl acrylate and 2,2,2-trifluoroethyl methacrylate copolymers were investigated in terms of hydrophobicity and sliding behavior of liquid droplets. The hydrophobicity of fluorinated latex films evaluated from water contact angle was closely related to the chemical composition of the surface. On the other hand, the sliding angle of liquid droplets was not directly proportional to the hydrophobicity or oleophobicity of the latex films in the present study. Although the hydrophobicity of copolymer latex films was significantly enhanced by adding small amount of highly fluorinated heptadecafluorodecyl acrylate, it made water droplets rather difficult to slide down on an inclined surface. The sliding angle of water droplet was quite sensitive to the preparation methods, namely, batch and semicontinuous emulsion polymerizations in contrast to the hydrophobicity. The surface morphology and roughness of the latex films were found to be important to explain the observations.

Introduction

Surface properties of materials are usually governed by the structure and chemical composition of the outermost surface layer and, thus, quite different from the bulk properties. One of prevailing strategies for reducing surface energy of materials is to utilize surface modification agent without altering their bulk properties. Among others, fluorinated polymers are widely used for this purpose due to their extremely low surface energy. In addition, the incorporation of fluorine atoms into the polymer structure results in other peculiar properties such as low refractive index, low friction coefficient, and chemical resistance.[1] Water and oil repellents for the textile, surface protection of stone and polymer films, mold releasing agent, molecular lubricant, and biofouling release coating, just to name a few, represent the typical applications of fluorinated polymers as surface modification agents.[2−8]

In particular, polymers with long side chains composed of a perfluoroalkyl group ($-C_nF_{2n+1}$) have received a great deal of attention. The conformational arrangement, distribution, and orientation of perfluoroalkyl side chains and their packing at the air/solid interface have been considered as a decisive parameter affecting the performance of the coating.[9−14] A number of methods have been proposed to achieve the highest surface density of $-CF_3$ terminal group at the interface. For example, the liquid crystalline ordering of perfluoroalkyl side chains can be enhanced by appropriate synthesis of segmented,[15] block,[16−20] and graft[21,22] copolymer structures that favor the surface segregation of the highly fluorinated portions of the polymer.

From a practical point of view, it is advantageous to synthesize and handle perfluorinated polymers as aqueous dispersions in process due to their notoriously low solubility in common organic solvents. Perfluorinated (meth)acrylates are suitable to produce latex particles, which afford fluorinated surface coatings during film formation, by emulsion polymerization. However, the perfluoroalkyl acrylate homopolymer exhibits some deteriorated properties on water and oil repellency. Therefore, in common practice, some auxiliary comonomers are necessary with perfluoroalkyl acrylate in order to improve the adhesion of particles to the substrates and to make coatings more durable by preventing self-dewetting which has been observed in homopolymers.[23] Although numerous research articles describing the preparation of perfluorinated polymers in solution and their surface properties have appeared in the literature, the preparation and film formation of fluorinated latex particles have been paid attention very recently despite their industrial importance.[24−31]

In the present study, we describe the surface properties of fluorinated latex films in terms of hydrophobicity and sliding behavior of liquid droplets. Little is known about the sliding behavior of liquid droplets on the latex films containing perfluoroalkyl groups. The hydrophobicity of the surface has been measured generally by the water contact angle. Under the assumption that the hydrophobicity is related to the work of adhesion,[32] the higher the water contact angle is, the more hydrophobic surface will be. On the other hand, the repellency of the surface, representing the rolling off or sliding down of liquid droplets on the surface, is also a useful concept to characterize the surface. The sliding behavior of liquid droplet has been evaluated conventionally from the so-called sliding angle, at which a liquid droplet with certain weight begins to slide down on the inclined plate. It has been well-known that the sliding behavior of liquid droplets does not always depend on the hydrophobicity of the surface, but on the existence of microscopic hindrance resulting from surface roughness or heterogeneity of chemical composition which produces the contact angle hysteresis.[33,34] For example, the sliding angles of water droplets on the less hydrophobic poly(dimethylsiloxane) are much lower than those on the more hydrophobic poly(perfluoroalkyl acrylate).[35] It means that the removal of water droplets is much easier on the poly(dimethylsiloxane) surface. As we shall see

---

* Corresponding author. FAX: +82-42-860-7590; e-mail: jongwook@krict.re.kr.

10.1021/ma0488764 CCC: $30.25

shortly, the sliding angle measurements are very sensitive to the surface conditions. We also discuss the morphology and chemical composition of latex film surfaces to elucidate the sliding behavior of liquid droplets as well as the bulk properties of the latex particles.

Experimental Section

Materials. Fluorinated monomers containing a $-CF_3$ terminal group in their side chains, heptadecafluorodecyl acrylate ($CH_2 = CHCOO(CH_2)_2C_8F_{17}$, FA) and 2,2,2-trifluoroethyl methacrylate ($CH_2 = C(CH_3)COOCH_2CF_3$, TFEMA), were purchased from Clariant and Lancaster, respectively. Cetyltrimethylammonium chloride (25 wt % solution in water, cationic surfactant, CTAC) and 1-dodecanethiol (chain transfer agent, DT) were purchased from Aldrich. Commercial grade of 2,2′-azobis(2-methylpropionamidine) dihydrochloride (initiator, V-50) was obtained from Wako. All materials were used without further purification. Water was purified by a Milli-Q system (Millipore).

Preparation of Latex Particles. The fluorinated latex particles were prepared from both the batch and semicontinuous emulsion polymerizations. For batch type emulsion polymerizations, 0.6 g of CTAC was dissolved in 150 g of water, and then 25.8 g of monomer (or monomer mixture) and 0.2 g of DT were added to the surfactant solution. The mixture was emulsified by ultrasonication and transferred into the reactor. Nitrogen gas was bubbled through the emulsified mixture for 30 min. 0.1 g of V-50 dissolved in 1 g of water was added when the temperature of reaction mixture attained 65 °C in an oil bath. The polymerization lasted for at least 6 h. The fluorinated copolymer latex particles were also prepared by semicontinuous emulsion polymerizations. In those cases, 0.2 g of DT was added to 25.8 g of monomer mixture with desired composition at first. 0.15 g of CTAC and 2.6 g of monomer mixture were added to 100 g of water and then emulsified by ultrasonication. After purging nitrogen gas and elevating the temperature to 65 °C, 0.1 g of V-50 dissolved in 1 g of water was added to the reaction mixture. 20 min later, a preemulsion consisting of 23.4 g of monomer mixture, 0.45 g of CTAC, and 50 g of water was dropped into the reactor by using a syringe pump at a rate of 20 mL/h. After completion of monomer feeding, the reaction lasted for another 3 h.

Characterization of Latex Particles. The monomer conversions were measured gravimetrically. The intensity-averaged hydrodynamic radii of latex particles were determined by photon correlation spectroscopy (Zetasizer 3000HS, Malvern). The intensity fluctuations of scattered light (He−Ne laser, 633 nm) were measured with a photon correlator at a fixed angle of 90°. To obtain dried samples, the latex particles were precipitated in 0.1 M sodium chloride solution. The precipitants were washed with water and ethanol several times after filtration. Finally, the samples were dried in reduced pressure at room temperature. The thermal behavior of dried latex samples was observed by a differential scanning calorimeter (DSC Q1000, TA Instruments) from −50 to 150 °C at a heating rate of 10 °C/min after quenching the samples at 150 °C. Wide-angle X-ray diffraction (WAXD) patterns were measured at room temperature with an X-ray diffractometer (D/MAX-2000, Rigaku), using monochromatic Cu Kα radiation (40 kV, 40 mA). The chemical compositions of the latex particles were determined by ^1H NMR (Bruker DPX300) using $CDCl_3$ and, if necessary, 1,1,2-trichlorotrifluoroethane as solvents.

Latex Film Formation. Latex films were prepared by spreading diluted latexes (∼1 wt % solid) directly on precleaned glass slides. The films were allowed to dry at room temperature under the covered Petri dish. After annealing at 130 °C for 24 h, transparent latex films were produced. However, the effect of surfactant added during the polymerization process on the surface properties could not be ruled out at that moment. For example, the water contact angle on the FA homopolymer latex film was considerably lower than literature values. Thus, latex films were rinsed with running water thoroughly and annealed again at 130 °C for another 24 h. By doing so, the effect of presumable surfactant segregation at the air/solid interface during film formation could be minimized. It has been confirmed that further purification did not influence the water contact angle anymore. Solvent-borne films of FA and TFEMA homopolymers were also prepared by spin-coating on the glass slide. After evaporating the solvent, the films were annealed at 130 °C for 24 h before subsequent analyses. For X-ray photoelectron spectroscopy (XPS) and atomic force microscopy (AFM) experiments, the latex films were prepared by following the same procedure except that the films were casted on smaller glass slides 10 mm × 10 mm in dimension.

Table 1. Characteristics of Heptadecafluorodecyl Acrylate (FA)/2,2,2-Trifluoroethyl Methacrylate (TFEMA) Copolymer Latexes Prepared by Batch and Semicontinuous Emulsion Polymerizations[a]

sample[b]	FA (wt %)[c]	FA (mol %)[d]	solid content (%)	particle size (nm)
PTFEMA	0	0.0 (0.0)	14.3	90
PFA	100	100.0 (100.0)	14.5	167
B-15	15	5.2 (5.0)	14.6	83
B-30	30	11.9 (12.0)	14.5	92
B-50	50	25.0 (25.0)	14.3	79
B-75	75	47.4 (50.0)	13.9	114
SC-15	15	5.1 (5.0)	14.2	108
SC-30	30	10.7 (12.0)	13.6	110
SC-50	50	23.7 (25.0)	13.9	110
SC-75	75	44.5 (50.0)	12.9	126

[a] The reaction mixture consists of 25.8 g of monomer (or monomer mixture), 0.6 g of cetyltrimethylammnium chloride, 0.2 g of 1-dodecanethiol, and 150 g of water in all experimental runs. [b] B and SC in the sample names denote batch and semicontinuous emulsion polymerizations, respectively. PFA and PTFEMA homopolymer latexes were prepared by batch emulsion polymerization. [c] The weight fraction of FA in the monomer mixtures. [d] The mole fraction of FA in the latex particles determined by ^1H NMR. Theoretical mole fraction of FA is shown in parentheses.

Characterization of Latex Films. Contact angle measurements were performed on a Rame-Hart goniometer. The static contact angles of wetting liquids were obtained from an average of several drops, and 10 μL of wetting liquid was used for each measurement. The sliding angles of liquid droplets were measured with a homemade apparatus. The coated glass slide was positioned on a horizontal plate, and the liquid droplet of known volume was formed by micropipet. The plate was inclined by the stepping motor with a fixed rate of 1°/s. The motor was stopped automatically when the motion of the droplet was detected. The chemical compositions of surfaces were determined by XPS (ESCA Lab 2000, VG Scientific) with a Mg Kα X-ray source. The X-ray gun was operated at 12 kV and 10 mA, and the analyzer chamber pressure was 10^{-8}mbar. The takeoff angle was fixed at 90°. AFM experiments were performed using a Nanoscope IV (Digital Instruments) in order to observe the surface morphology and to measure surface roughness of latex films. Images were acquired under ambient conditions in tapping mode.

Results and Discussion

Synthesis of Latex Particles. The basic characteristics of the resulting latex particles are summarized in Table 1. In all cases, the solid contents are close to the expected value of 14.9 wt %. Therefore, it is anticipated that the chemical compositions of latex particles are not much different from those of monomers. The incorporation of both fluorinated monomers into the latex particles was confirmed by ^1H NMR by evaluating the peak intensities at 4.3 ppm ($-OCH_2$) and 2.5 ppm ($-OCH_2CH_2$). The hydrodynamic radii of latex particles prepared from semicontinuous emulsion polymerization increase gradually with FA fraction in the

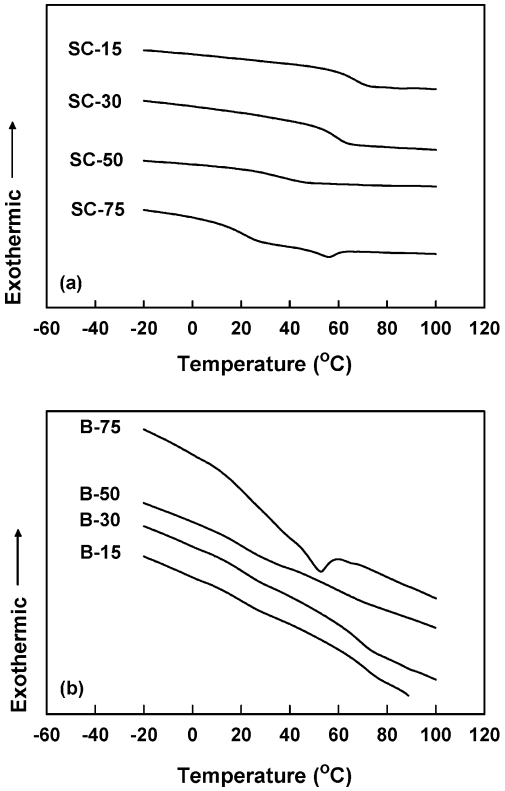

Figure 1. DSC thermograms of copolymer latexes prepared from (a) semicontinuous and (b) batch emulsion polymerizations.

feed, while batch emulsion polymerization does not show any tendency on the particle size under the present polymerization conditions.

The chemical composition of latex particles determined by ^{1}H NMR, however, does not provide the information on the microstructure of polymer chains in detail. The possibility that a minor amount of homopolymer is coexisted with copolymer cannot be excluded. Thus, DSC and WAXD experiments were carried out in order to examine the homogeneity of the copolymers. The presence of FA homopolymers in latex blends is able to produce noticeable effects on the thermal and crystalline behaviors.[30] It has been known that PFA homopolymer is semicrystalline showing the first-order transition at 75 °C, whereas the TFEMA homopolymer is amorphous with one glass transition temperature at 75 °C. More complex thermal behavior was observed in copolymer latexes as reproduced in Figure 1. At first, the copolymer latexes prepared by semicontinuous emulsion polymerization show usually one glass transition temperature except SC-75 in which the largest amount of FA is incorporated. In that case, one glass transition temperature around 20 °C and one broad first-order transition at 55 °C are observed. The glass transition temperature decreases slightly as increasing FA fraction in the copolymers. The thermal behavior of copolymer latexes prepared by batch emulsion polymerization is a little different from those prepared semicontinuously with the same compositions. When the FA fraction in copolymers is less than 50 wt %, two distinctive glass transition temperatures at around 20 and 70 °C are detected. In addition, a more pronounced first-order transition is observed in B-75. The thermal behavior of latex particles thus reveals that the microstructure of the latex particles is influenced very much by the preparation method.

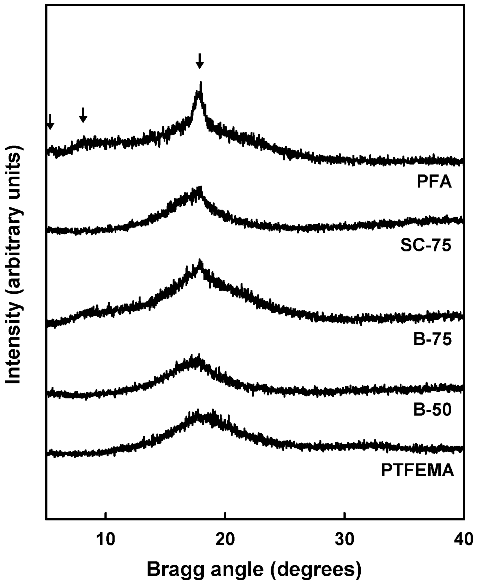

Figure 2. Powder X-ray diffraction spectra for the latex particles. For the PFA homopolymer, arrows stand for the Bragg peaks observed at $2\theta = 5.2$, 8.0, and 17.7°, corresponding to 16.8, 11.0, and 5.0 Å in Bragg spacing, respectively.

The homogeneity of copolymer chains was further examined by WAXD experiments. The diffraction spectra obtained at room temperature are shown in Figure 2. The PTFEMA spectrum does not show a sharp peak, merely a diffusion band at 4.85 Å, characteristic of an amorphous state as expected. The crystallinity observed in FA homopolymer is attributed to the layer structure of side chains. The small-angle peaks ($2\theta < 10°$) are corresponding to successive diffraction orders and characteristics of a smectic B lamellar order.[9,13] The crystalline order between adjacent perfluoroalkyl side chains results in a sharp peak around $2\theta \sim 18°$. Among the copolymer samples considered in this study, a Bragg peak at 5.0 Å can be found only in the samples containing the highest fraction of perfluoroalkyl groups, B-75 and SC-75. One thing to note is that, in the case of B-75, the diffraction spectrum is quite similar to that of perfluoroalkyl homopolymer, and long-range lamellar crystalline order is more pronounced compared with SC-75. This result is in agreement with thermal behavior of latex particles shown in Figure 1. On the basis of the DSC and WAXD results, it can be assumed that the latex particles prepared from batch emulsion polymerization consists of TFEMA-rich and FA-rich copolymers, even though the formation of homopolymers is not evident. In contrast, the semicontinuous emulsion polymerization seems to produce chemically homogeneous latex particles.

The monomer transport from the emulsion droplets to the growing particles is essential to making polymer latexes by conventional emulsion polymerization. Because of the heterogeneous nature of the reaction, the partitioning of the different monomers between the organic and aqueous phases is a crucial factor to determine the composition of the copolymer chains formed. As a result, depending on the monomer polarity and reactivity as well as solubility in water, statistical copolymerization in emulsion polymerization is doubtful. In particular, because of the extraordinarily low solubility in water, heterogeneous particles are usually observed in emulsion copolymerization of perfluorinated monomers with hydrocarbon comonomers.[29] Another

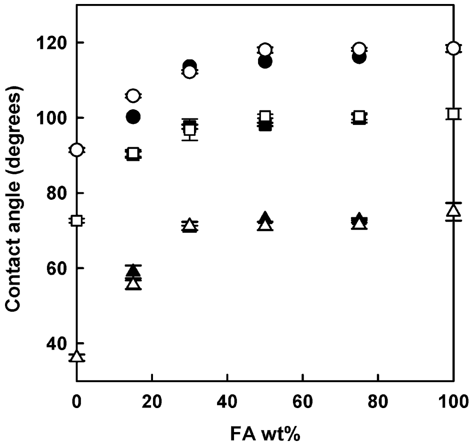

Figure 3. Static contact angles of water (circles), diiodomethane (squares), and *n*-hexadecane (triangles) on the latex films prepared from batch (open symbols) and semicontinuous emulsion polymerizations (filled symbols).

recent study has shown that the copolymer structure becomes rather blocky by varying the type of polymerization from solution to emulsion.[36]

The uniformity of the copolymer composition also depends on the monomer feeding conditions. In semicontinuous emulsion polymerization, the monomers added show instantaneous conversion under the monomer-starved condition. If the comonomer mixture is completely polymerized immediately upon entering the reactor, then the copolymer formed must have the same overall composition as that of the comonomer mixture added. Thus, it is possible to produce copolymers of relatively uniform composition.[37] The different monomer feeding conditions produce significant effects on the surface properties of resulting polymers even in the case of solution copolymerization of fluorocarbon and hydrocarbon comonomers. For example, at a given weight percent of perfluoroalkyl methacrylate in the polymer, the single shot feeding of monomer mixture produces the higher water and *n*-hexadecane contact angles compared with continuous feeding. According to Thomas et al., the difference in surface properties can be explained by considering polymer architecture.[38] The single shot feeding of monomer mixture results in more blocky polymers, and thus, the perfluoroalkyl groups from several polymer chains are able to form domains of appreciable surface area fractions.

The surface segregation of $-CF_3$ terminal groups at the interface, which is the main reason for the hydrophobicity of polymers containing perfluoroalkyl groups, is also influenced by various effects such as chain length, blockiness, and degree of incorporation of the fluorinated monomer. On the basis of the DSC and WAXD results, the fluorinated copolymer latex particles considered in the present study can be assumed to have random structure macroscopically, but it can be also assumed that there is a noticeable difference in polymer architecture depending on the preparation method. Consequently, it is expected that the polymer architecture, for instance the blockiness by leading to microphase separation of the bulk, affects surface properties of latex films as discussed in the following section.

Surface Properties of Latex Films. Figure 3 shows the water and diiodomethane contact angles on the films of latex particles prepared by batch and semicontinuous emulsion polymerizations. In addition, the *n*-hexadecane contact angles are also included as an index of oleophobicity. As expected, the contact angles of wetting liquids are enhanced initially with increasing the amount of FA in the copolymers. That is, both the hydrophobicity and oleophobicity are improved by incorporating heptadecafluorodecyl groups into the latex films. There is no further increase of contact angles when the FA fraction exceeds about 50 wt %.

The surface free energy of solid can be calculated from the contact angles of two wetting liquids having known values of polar (γ^{p}) and dispersive (γ^{d}) components of surface energy as follows:[39]

$$\gamma_{L}(1 + \cos \theta) = 2(\gamma_{s}^{d}\gamma_{L}^{d})^{1/2} + 2(\gamma_{s}^{p}\gamma_{L}^{p})^{1/2} \qquad (1)$$

In this semiempirical equation, subscripts L and s refer to the wetting liquid and the solid, respectively, and θ is the contact angle of a sessile droplet in the equilibrium state. The surface energy, γ, is defined as the summation of the polar and dispersive components. While water ($\gamma_{L}^{d} = 21.7$ mN/m, $\gamma_{L}^{p} = 51.8$ mN/m at 22 °C) and diiodomethane ($\gamma_{L}^{d} = 48.1$ mN/m, $\gamma_{L}^{p} = 1.3$ mN/m) have been used generally to estimate γ_{s}^{d} and γ_{s}^{p}, it is also possible to use one *n*-alkane as a wetting liquid.[13] We used *n*-hexadecane ($\gamma_{L}^{d} = 27.6$ mN/m, $\gamma_{L}^{p} = 0$ mN/m) as an apolar wetting liquid.

Given in Table 2 are the polar and dispersive components and surface free energy of the latex films calculated from geometric mean approximation in eq 1. In the present study, since the latex particles were prepared from emulsion polymerization, surfactant molecules resided in the films inevitably. The presence of the surfactant molecules at the air/solid interface is able to influence the surface properties, for instance, through the surface solubilization of wetting liquids.[40] As mentioned previously, to remove surfactant, the surface properties of latex films were examined after rinsing with water and reannealing, and thus, the effect of surfactant segregated on the surface was assumed to be negligible. It was confirmed by comparing measured surface energies of homopolymer latex films with literature values. The surface free energy of PFA estimated from water and diiodomethane as wetting liquids is 8.5 mN/m, as shown in Table 2. This value is slightly higher than the surface energy measured on the surface where the $-CF_3$ groups are regularly aligned and hexagonally packed[41] and is consistent with 7−10 mN/m reported in the literature on the PFA surface prepared from solution polymerization.[13,42] The successful removal of surfactant molecules was also confirmed from XPS measurements. There was no sign of N_{1s} at least in the outmost layer of the latex films.

The effect of surface solubilization on the surface energy measurement can be appreciated by selecting *n*-hexadecane as a wetting liquid.[13,43] As can be found in Table 2, the surface energy of PFA estimated from water and *n*-hexadecane contact angles is 11.2 mN/m. It is well-known that the low molecular weight *n*-alkane is usually adsorbed or solubilized on the surface. This is problematic especially in the determination of the critical surface tension by Zisman's plot since the spreading pressure, which is neglected generally, is influenced greatly by dissolution of wetting liquid. In the case of higher molecular weight *n*-alkane, such as *n*-hexadecane, it has been accepted that the dissolution effect is negligible. However, our measurement exhibited that there is some difference in the estimated surface energies of PFA latex films depending on the

Table 2. Surface Energies of Latex Films Estimated from Eq 1

	water/diiodomethane pair			water/*n*-hexadecane pair		
	γ_s^d (mN/m)	γ_s^p (mN/m)	γ_s (mN/m)	γ_s^d (mN/m)	γ_s^p (mN/m)	γ_s (mN/m)
PFA	7.8	0.7	8.5	10.9	0.3	11.2
PTFEMA	18.9	4.6	23.5	22.5	3.5	26.0
B-15	11.1	2.4	13.5	16.9	1.0	17.9
B-30	8.9	1.5	10.4	12.1	0.8	12.9
B-50	8.0	0.7	8.7	12.1	0.2	12.3
B-75	8.0	0.7	8.7	11.9	0.2	12.1
SC-15	10.7	4.3	15.0	15.8	2.5	18.3
SC-30	8.7	1.3	10.0	12.2	0.6	12.8
SC-50	8.6	1.1	9.7	11.5	0.5	12.0
SC-75	8.0	1.0	9.0	11.6	0.4	12.0

wetting liquids, and this might reflect the influence of the spreading pressure, which is far from the current research scope.

The surface energy of PTFEMA homopolymer latex films is 23.5−26.0 mN/m depending on the selection of wetting liquids, much higher than that of PFA latex film. The surface energy of copolymer latex films decreases monotonically as increasing the FA fraction in the latex particles up to 50 wt %. Further reduction of surface energy is not observed with FA fraction. In many cases, the surface energy of random copolymers is linearly proportional to the molar fraction of their monomer units. However, the surface energy of copolymers containing fluorinated monomers is varied in a nonlinear way, that is, a small fraction of fluorinated monomers induces a significant reduction of surface energy mainly due to the surface segregation of fluorinated portion of the polymer chains. It can be also found in Figure 3 that there is no considerable difference in surface energies between latex films prepared from different polymerization methods.

While the water contact angle has been commonly used as a criterion for the hydrophobicity of the surface, this alone is insufficient for the evaluation of the sliding behavior of water droplets on surfaces. In some application fields, the removal of liquid droplets on the surface by rolling off or sliding down is more important rather than the hydrophobicity itself. The sliding angles of water and *n*-hexadecane droplets on the PFA and PTFEMA homopolymer latex films are represented in Figure 4a as a function of droplet volume. As observed previously, the PFA homopolymer latex film is more hydrophobic and oleophobic than PTFEMA on the basis of the contact angle measurements. However, the sliding behavior of liquid droplets is almost the same on two latex films. The sliding angles of water droplets on the PTFEMA surface are even consistently lower than those on the PFA surface. *n*-Hexadecane droplets are more easily slide down on the PFA surface, but the difference is not significant. The solid line included in the plot stands for the literature value measured on the PFA homopolymer film prepared by solution polymerization,[35] which is in good agreement with our result.

The sliding behavior of liquid droplets on an inclined surface can be analyzed by taking into account the capillary force retaining droplet. After some mathematical manipulations, Carre and Shanahan[44] proposed the following relationship between the volume of liquid droplet V_i and sliding angle α_i

$$V_i^{2/3}\sin\alpha_i = \left[\frac{6\pi^2}{t(t^2+3)}\right]^{1/3}\frac{\gamma_L}{2\rho g}(\cos\theta_R - \cos\theta_A) = K(\text{const}) \quad (2)$$

in which ρ is the density of the droplet, g is the gravity, and $t = \tan(\theta/2)$. It can be clearly seen that the sliding angle is related to not only the static contact angle but also the contact angle hysteresis describing the difference between advancing (θ_A) and receding (θ_R) contact angles. Since the right-hand side of the equation is a constant for a given liquid/solid system, the product $V_i^{2/3}\sin\alpha_i$ should be constant for a given system. As shown in Figure 4b, the constancy of $V_i^{2/3}\sin\alpha_i$ as a function of V_i is clearly observed within experimental errors.

In Figure 5, the sliding angles of water droplets on the homopolymer films prepared by different film-forming methods are depicted. The preparation method does not alter the sliding angle of water droplets. The constancy of $V_i^{2/3}\sin\alpha_i$ is preserved in all cases. It can be confirmed again that the surfactant molecules were removed successfully from latex films.

The sliding angles of a 40 μL water droplet on the copolymer latex films are shown in Figure 6. Interest-

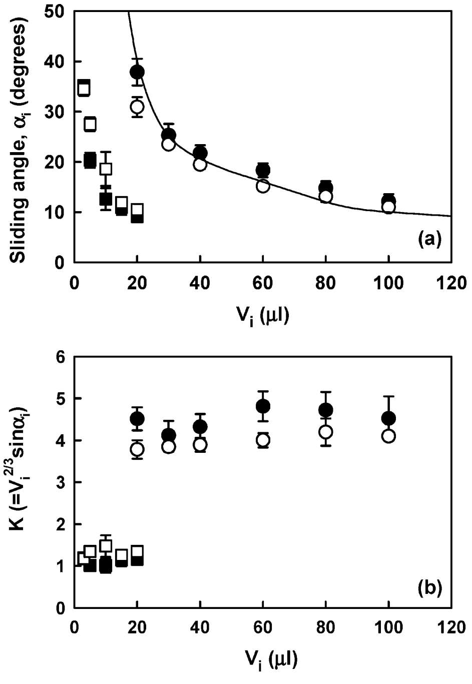

Figure 4. (a) Sliding angles of water (circles) and *n*-hexadecane (squares) droplets and (b) K (= $V_i^{2/3}\sin\alpha_i$) as a function of droplet volume (V_i) on the latex films prepared from heptadecafluorodecyl acrylate (filled symbols) and 2,2,2-trifluoroethyl methacrylate (open symbols) homopolymers. (b) K = 4.50 ± 0.40 and 3.93 ± 0.22 for the water droplets and K = 1.10 ± 0.14 and 1.33 ± 0.16 for the *n*-hexadecane droplets on the heptadecafluorodecyl acrylate and 2,2,2-trifluoroethyl methacrylate homopolymer latex films, respectively. The solid line in (a) stands for the literature data for the sliding angle of water droplets on FA homopolymer film produced from solvent casting.[35]

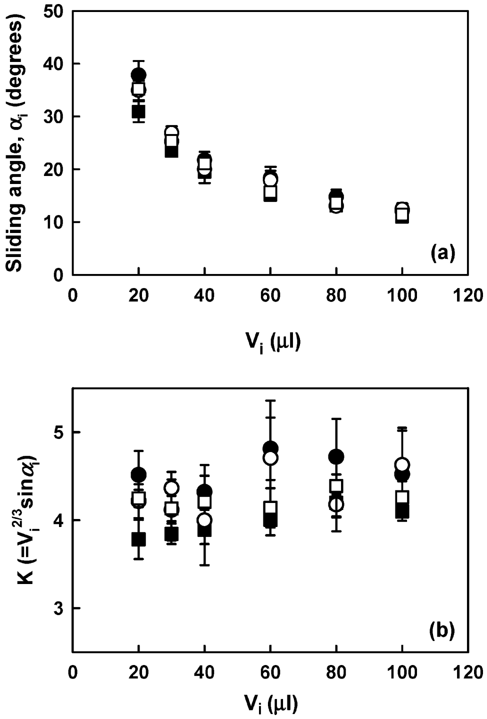

Figure 5. (a) Sliding angles and (b) K (= $V_i^{2/3}$ sin α_i) as a function of droplet volume (V_i) of water droplets on the heptadecafluorodecyl acrylate (circles) and 2,2,2-trifluoroethyl methacrylate (squares) homopolymer films prepared from latex particles (filled symbols) and solvent-casting (open symbols). (b) $K = 4.50 \pm 0.40$ and 4.35 ± 0.43 for the heptadecafluorodecyl acrylate films and $K = 3.93 \pm 0.22$ and 4.23 ± 0.20 for the 2,2,2-trifluoroethyl methacrylate homopolymer films prepared from latex particles and solvent casting, respectively.

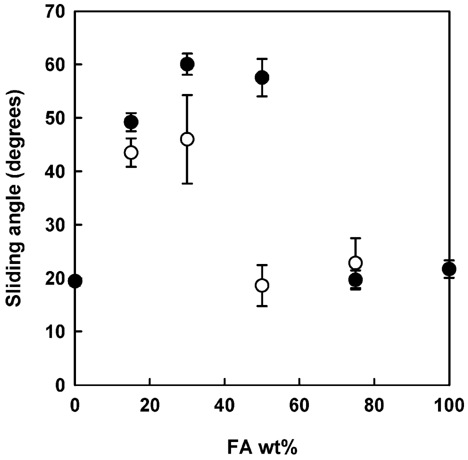

Figure 6. Sliding angles of 40 μL water droplets on the heptadecafluorodecyl acrylate/2,2,2-trifluoroethyl methacrylate copolymer latex films as a function of FA wt %. Open and filled symbols stand for the latex films prepared from semicontinuous and batch emulsion polymerizations, respectively.

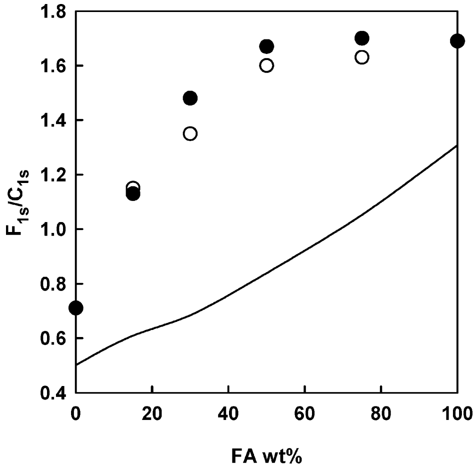

Figure 7. F_{1s}/C_{1s} atomic ratio determined by XPS experiments as a function of FA wt % in the latex particles. Open and filled symbols stand for the latex films prepared from the semicontinuous and batch emulsion polymerizations. The solid line denotes the theoretical atomic ratio estimated from monomer compositions.

ingly, it is not advantageous to introduce heptadecafluorodecyl groups into the latex films from the viewpoint of sliding angle of water droplets unlike the hydrophobicity. The water contact angle increased so that the surface energy decreased with FA fraction in the copolymers up to 50 wt % as represented in Figure 3. However, the sliding angle of water droplets increases on the contrary as decreasing surface energy of latex films and exhibits a maximum when the FA fraction is about 30 wt %. In other words, the incorporation of FA into the copolymers makes the latex film more hydrophobic but the removal of water droplets on the surface more difficult. Further increasing of FA fraction is not effective to reduce surface energy but sliding angle of water. Another thing to note is that the sliding angles of water droplets are much lower on the latex films prepared from semicontinuous emulsion polymerization, although the surface energies are almost the same regardless of the copolymerization methods.

In all experiments, the sliding droplets kept their rounded shape without breakup. On the less hydrophobic surface where the contact angle is low, a sliding droplet may deform into a cusped shape with tail from a rounded shape.[45] Eventually tiny droplets are released behind the sliding main droplet by singularity similar to Rayleigh instability observed in extending or relaxing droplets. The resulting small droplets remain pinned on an inclined surface. Thus, it is obvious that the surface must be sufficiently hydrophobic in order to remove the droplet completely by inclination of the surface. As predicted in eq 2, for a given value of contact angle hysteresis, it is true that the sliding angle decreases as increasing advancing contact angle or, equivalently, hydrophobicity of the surface.[46] However, in real situations, the higher hydrophobicity does not always ensure the lower sliding angle. A lot of exceptional results have been found mainly due to the fact that the contact angle hysteresis is influenced by many other causes such as surface roughness, chemical heterogeneity of the surface, mechanical irreversibility, and molecular rearrangement at the surface.[47,48] In this study, the chemical composition and roughness of latex film surfaces are mainly considered.

The chemical composition of the outmost layer of latex films measured with XPS experiments is represented in Figure 7. Because of the surface segregation of hydrophobic perfluoroalkyl groups, the F_{1s}/C_{1s} ratio is not proportional to the FA fraction in copolymer latex particles. In all cases, the ratio is higher than that of theoretical value determined from monomer composition. Even in the homopolymer latex films, the fluorine content is enhanced at the air/solid interface as observed in previous research.[49–51] As can be found in Figure 7, the small amount of FA induced rapid enhancement of F_{1s}/C_{1s} ratio in the copolymers. The surface chemical

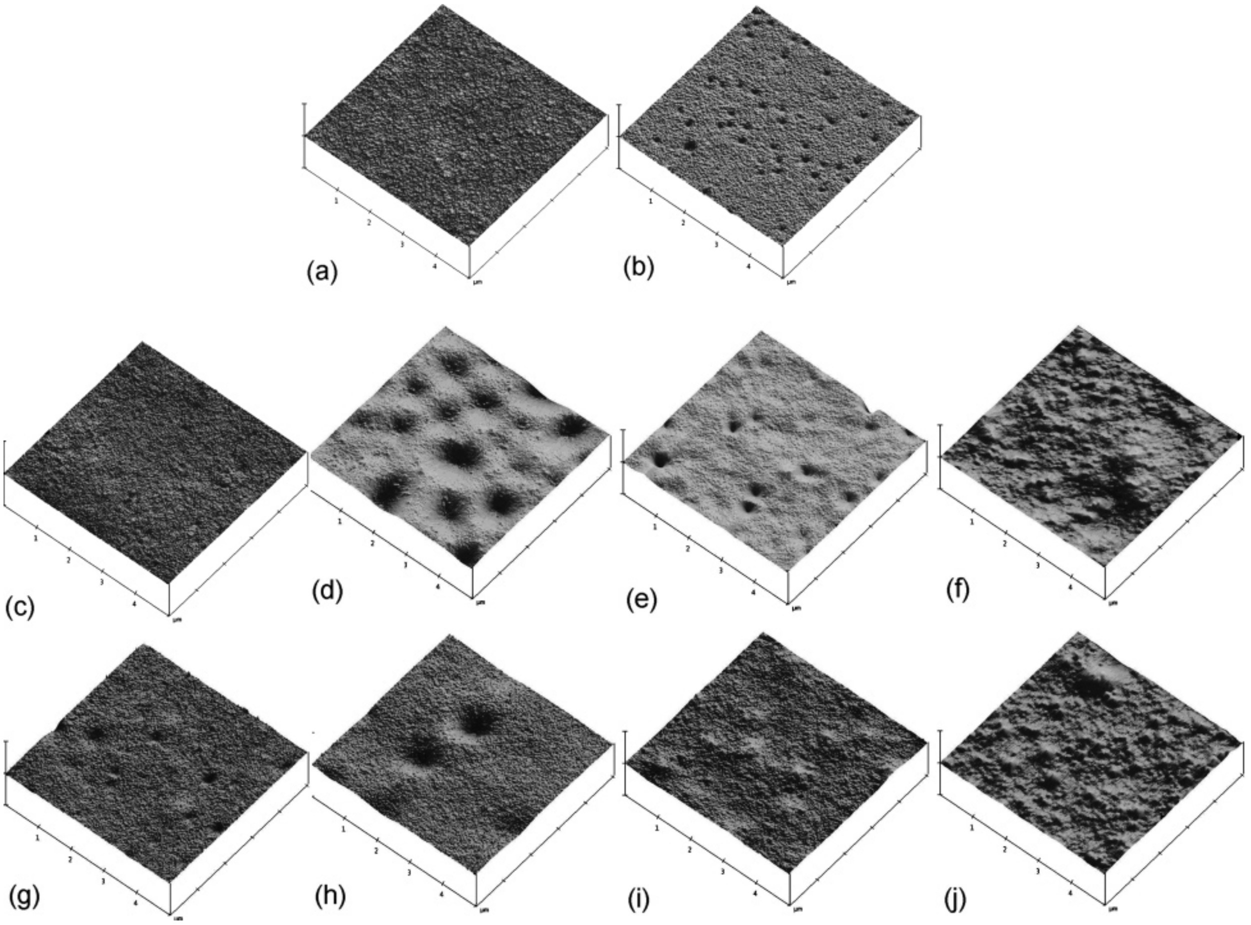

Figure 8. AFM images of latex films in tapping mode in 5 μm × 5 μm area: (a) PTFEMA, (b) PFA, (c) B-15, (d) B-30, (e) B-50, (f) B-75, (g) SC-15, (h) SC-30, (i) SC-50, and (j) SC-75.

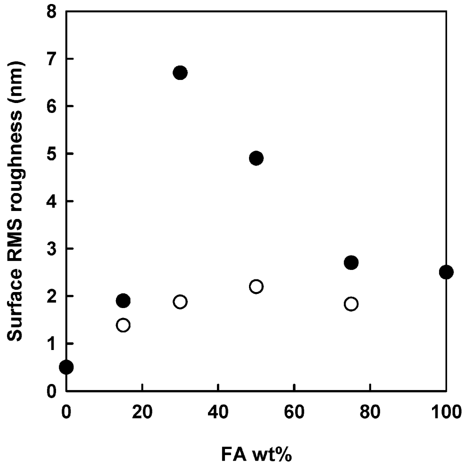

Figure 9. Root-mean-square surface roughness measured from AFM experiments in 5 μm × 5 μm area as a function of FA weight fraction in the copolymers. Open and filled symbols represent the latex films prepared from semicontinuous and batch emulsion polymerizations, respectively.

composition of the latex films containing more than 50 wt % of FA becomes similar to that of PFA homopolymer. The fluorine content is slightly higher on the latex films prepared from batch emulsion polymerization. The XPS results are coincident exactly with the surface energy measurements. Therefore, it can be concluded that the hydrophobicity and oleophobicity of the latex films are governed by the fluorine content on the surface. However, the XPS results do not provide any explanation on the sliding behavior of the liquid droplets on the latex films.

The surface roughness plays a significant role in surface properties. In the case of hydrophobic surface, the apparent water contact angle is enhanced by surface roughness. The so-called "Lotus effect" is a well-known example of the combined effect of hydrophobicity and surface roughness.[52] On that surface, the water contact angle exceeds 150° while the contact angle hysteresis remains small. As a consequence, the surface is almost fully nonwettable, and the water droplet has a spherical shape and rolls down on the inclined surface instead of sliding down. Usually surface roughness of several tens of nanometers is required to produce such a superhydrophobic surface. On the other hand, a slight increase of surface roughness leads to larger contact angle hysteresis, although the apparent contact angle increases.

To explain the sliding behavior of water droplets observed in Figure 6, the surface morphology and roughness of the latex films were investigated by AFM. In Figures 8 and 9, the surface morphology and root-mean-square (RMS) roughness of latex films are shown. Depending on the FA fraction in the copolymers, the surface morphology is varied significantly. At first, let us consider the latex films prepared from batch emulsion polymerization (Figure 8c−f and filled symbols in Figure 9). The addition of FA into the copolymers is responsible for the formation of much rougher latex films. The AFM image of B-30 is similar to microphase separation observed usually in block copolymers or immiscible polymer blends. Copolymer latex films containing more than 75 wt % of FA have similar surface roughness with PFA homopolymer. Also, it can be found that there is a large difference in surface morphology and roughness between latex films prepared by batch and semicontinuous emulsion polymerizations. The surface roughness of the latex films exhibits the identical tendency with the sliding behavior of the water droplets in cases of batch emulsion polymerization in particular.

Unfortunately, it was hardly possible to control the surface roughness and morphology separately in the present study. Thus, it is not sure that the surface roughness as small as 7 nm in RMS alone is a sufficient condition to govern the sliding behavior of the liquid droplets. Moreover, in the case of latex films prepared from semicontinuous emulsion polymerization, the sliding angles of the water droplet were altered considerably by varying FA fraction in copolymers while the surface roughness was not very much. As discussed briefly, the architecture in copolymer chain can be influenced by the polymerization procedure. Compared with semicontinuous one, the batch emulsion polymerization seems to produce rather blocky copolymers. The blockiness of the copolymer chains should affect the microstructure of the latex films and, thus, roughness of the films. This is responsible for the higher sliding angle of water droplet on the latex films prepared from batch emulsion polymerizations despite the fact that the bulk and surface compositions were almost the same in both cases.

Considering homopolymer latex films, the difference in surface roughness is only subtle, and the surface structure is anticipated to be homogeneous relatively compared with copolymer latex films. Thus, surface roughness and heterogeneity might be less important parameter to explain the nearly identical sliding behavior of liquid droplets on the homopolymer films possessing different hydrophobicity. In that case, other surface properties such as molecular interaction between surface and wetting liquid must be taken into account.[35]

Conclusions

A series of latex particles have been prepared by batch and semicontinuous emulsion polymerizations of fluorinated monomers, heptadecafluorodecyl acrylate and 2,2,2-trifluoroethyl methacrylate. The bulk properties such as thermal behavior and X-ray diffraction patterns of resulting latex particles were studied to examine the homogeneity of copolymer structure. Although there was no indication of homopolymer formation, noticeable differences in microstructure of copolymer chains were found depending on the polymerization methods. The batch emulsion polymerization seemed to produce the latex particles with more blocky structure. Further experiments were carried out to observe the effect of polymer architecture on the surface properties of latex films. The hydrophobicity and oleophobicity estimated from static contact angle measurements of water and *n*-hexadecane showed the same tendency with the surface chemical composition measured from XPS. As increasing the amount of heptadecafluorodecyl groups in the latex films, the contact angles of wetting liquids were increased, and consequently, surface energy was reduced. The effect of heptadecafluorodecyl groups incorporated into latex films was saturated when the amount of FA was exceeded to 50 wt %. The polymerization method produced little effect on the hydrophobicity, oleophobicity, or fluorine atomic fraction at the film surfaces. Sliding angles of water and *n*-hexadecane were also measured on the latex films. Interestingly, both the wetting liquids exhibited almost the same sliding behavior on the homopolymer films despite considerable differences in hydrophobicity and oleophobicity. Compared with homopolymer latex films, higher sliding angles of water droplet were observed in copolymer latex films. The increase of water sliding angle was much more considerable for the latex films prepared from batch emulsion polymerization, wherein the surface compositions of latex films were almost identical, but the surface morphology and roughness were quite different from latex films prepared from semicontinuous emulsion polymerization.

Acknowledgment. This work was supported by the National Research Laboratory Program (2000-N-NL-01-C0241) of the Korea Ministry of Science and Technology.

References and Notes

(1) Grainger, D. W.; Stewart, C. W. Fluorinated Coatings and Films; Motivation and Significance. In *Fluorinated Surfaces, Coatings, and Films*; Castner, D. G., Grainger, D. W., Eds.; ACS Symposium Series 787; American Chemical Society: Washington, DC, 2001; p 1.
(2) Chen, S.-I.; Sheu, Y. L.; Sheu, J.-L.; Lee, C.-T.; Lin, J. S. *J. Appl. Polym. Sci.* **1997**, *63*, 903−909.
(3) Furukawa, Y.; Kotera, M. *J. Appl. Polym. Sci.* **2003**, *87*, 1085−1091.
(4) Lazzari, M.; Aglietto, M.; Castelvetro, V.; Chiantore, O. *Chem. Mater.* **2001**, *13*, 2843−2849.
(5) Walters, K. B.; Schwark, D. W.; Hirt, D. E. *Langmuir* **2003**, *19*, 5851−5860.
(6) Thanawala, S. K.; Chaudhury, M. K. *Langmuir* **2000**, *16*, 1256−1260.
(7) Waltman, R. J.; Shieh, M. G. *Macromolecules* **2001**, *34*, 6776−6782.
(8) Schmidt, D. L.; Brady, R. F.; Lam, K.; Schmidt, D. C.; Chaudhury, M. K. *Langmuir* **2004**, *20*, 2830−2836.
(9) Volkov, V. V.; Platé, N. A.; Takahara, A.; Kajiyama, T.; Amaya, N.; Murata, Y. *Polymer* **1992**, *33*, 1316−1320.
(10) Shimizu, T.; Tanaka, Y.; Kutsumizu, S.; Yano, S. *Macromolecules* **1996**, *29*, 156−164.
(11) Genzer, J.; Sivaniah, E.; Kramer, E. J.; Wang, J.; Körner, H.; Char, K.; Ober, C. K.; DeKoven, B. M.; Bubeck, R. A.; Fischer, D. A.; Sambasivan, S. *Langmuir* **2000**, *16*, 1993−1997.
(12) Lüning, J.; Stöhr, J.; Song, K. Y.; Hawker, C. J.; Iodice, P.; Nguyen, C. V.; Yoon, D. Y. *Macromolecules* **2001**, *34*, 1128−1130.
(13) Corpart, J.-M.; Girault, S.; Juhué, D. *Langmuir* **2001**, *17*, 7237−7244.
(14) Fujimori, A.; Araki, T.; Nakahara, H.; Ito, E.; Hara, M.; Ishii, H.; Ouchi, Y.; Seki, K. *Langmuir* **2002**, *18*, 1437−1440.
(15) Chapman, T. M.; Marra, K. G. *Macromolecules* **1995**, *28*, 2081−2085.
(16) Ren, Y.; Lodge, T. P.; Hillmyer, M. A. *Macromolecules* **2001**, *34*, 4780−4787.
(17) Li, X.; Andruzzi, L.; Chiellini, E.; Galli, G.; Ober, C. K.; Hexemer, A.; Kramer, E. J.; Fischer, D. A. *Macromolecules* **2002**, *35*, 8078−8087.
(18) Zhang, Z. B.; Ying, S. K.; Hu, Q. H.; Xu, X. D. *J. Appl. Polym. Sci.* **2002**, *83*, 2625−2633.
(19) Hussain, H.; Budde, H.; Höring, S.; Busse, K.; Kressler, J. *Macromol. Chem. Phys.* **2002**, *203*, 2103-2112.
(20) Li, K.; Wu, P.; Han, Z. *Polymer* **2002**, *43*, 4079−4086.
(21) Park, I. J.; Lee, S.-B.; Choi, C. K. *Polymer* **1997**, *38*, 2523−2527.
(22) Park, I. J.; Lee, S.-B.; Choi, C. K. *Macromolecules* **1998**, *31*, 7555−7558.
(23) Sheiko, S.; Lermann, E.; Möller, M. *Langmuir* **1996**, *12*, 4015−4024.
(24) Pan, G.; Tse, A. S.; Kesavamoorthy, R.; Asher, S. A. *J. Am. Chem. Soc.* **1998**, *120*, 6518−6524.
(25) Linemann, R. F.; Malner, T. E.; Brandsch, R.; Bar, G. Ritter, W.; Mülhaupt, R. *Macromolecules* **1999**, *32*, 1715−1721.

(26) Thomas, R. R.; Lloyd, K. G.; Stika, K. M.; Stephanes, L. E.; Magallanes, G. S.; Dimonie, V. L.; Sudol, E. D.; El-Aasser, M. S. *Macromolecules* **2000**, *33*, 8828−8841.

(27) Castelvetro, V.; Ciargelli, F.; Francini, G.; Baglioni, P. *Macromol. Mater. Eng.* **2000**, *278*, 6−16.

(28) Koenderink, G. H.; Sacanna, S.; Pathmamanoharan, C.; Raşa, M.; Philipse, A. P. *Langmuir* **2001**, *17*, 6086−6093.

(29) Landfester, K.; Rothe, R.; Antonietti, M. *Macromolecules* **2002**, *35*, 1658−1662.

(30) Ha, J.-W.; Park, I. J.; Lee, S.-B.; Kim, D.-K. *Macromolecules* **2002**, *35*, 6811−6818.

(31) Ha, J.-W.; Park, I. J.; Kim, D.-K.; Kim, J.-H.; Lee, S.-B. *Surf. Sci.* **2003**, 532−535, 328−333.

(32) Adamson, A. W. *Physical Chemistry of Surfaces*, 4th ed.; Wiley: New York, 1982; Chapter 12.

(33) Anton, D. *Adv. Mater.* **1998**, *10*, 1197−1205.

(34) Della Volpe, C.; Siboni, S.; Morra, M. *Langmuir* **2002**, *18*, 1441−1444.

(35) Murase, H.; Fujibayashi, T. *Prog. Org. Coat.* **1997**, *31*, 97−104.

(36) de Crevoisier, G.; Fabre, P.; Leibler, L.; Tencé-Girault, S.; Corpart, J. M.; *Macromolecules* **2002**, *35*, 3880−3888.

(37) Lovell, P. A. Batch and Semi-batch Processes. In *Emulsion Polymerization and Emulsion Polymers*; Lovell, P. A., El-Aasser, M. S., Eds.; Wiley: New York, 1997; pp 239−276.

(38) Thomas, R. R.; Anton, D. R.; Graham, W. F.; Darmon, M. J.; Sauer, B. B.; Stika, K. M.; Swartzfager, D. G. *Macromolecules* **1997**, *30*, 2883−2890.

(39) Owens, D. K.; Wendt, R. C. *J. Appl. Polym. Sci.* **1969**, *13*, 1741−1747.

(40) Butler, L. N.; Fellows, C. M.; Gilbert, R. G. *Ind. Eng. Chem. Res.* **2003**, *42*, 456−464.

(41) Nishino, T.; Meguro, M.; Nakamae, K.; Matsushita, M.; Ueda, Y. *Langmuir* **1999**, *15*, 4321−4323.

(42) Graham, P.; Stone, M.; Thorpe, A.; Nevell, T. G.; Tsibouklis, J. *J. Fluorine Chem.* **2000**, *104*, 29−36.

(43) Schmidt, D. L.; DeKoven, B. M.; Coburn, C. E.; Potter, G. E.; Meyers, G. F.; Fischer, D. A. *Langmuir* **1996**, *12*, 518−529.

(44) Carre, A.; Shanahan, M. E. R. *J. Adhes.* **1995**, *49*, 177−185.

(45) Podgorski, T.; Flesselles, J.-M.; Limat, L. *Phys. Rev. Lett.* **2001**, *87*, 036102.

(46) Quéré, D. *Langmuir* **1998**, *14*, 2213−2216.

(47) Chaudhury, M. K.; Owen, M. J. *J. Phys. Chem.* **1993**, *97*, 5722−5726.

(48) Albenge, O.; Lacabanne, C.; Beguin, J.-D.; Koënen, A.; Evo, C. *Langmuir* **2002**, *18*, 8929−8932.

(49) Park, I. J.; Lee, S.-B.; Choi, C. K.; Kim, K.-J. *J. Colloid Interface Sci.* **1996**, *181*, 284−288.

(50) Tsibouklis, J.; Stone, M.; Thorpe, A. A.; Graham, P.; Nevell, T. G.; Ewen, R. J. *Langmuir* **1999**, *15*, 7076−7079.

(51) Takahashi, S.; Kasemura, T.; Asano, K. *Polymer* **1997**, *38*, 2107−2111.

(52) Blossey, R. *Nat. Mater.* **2003**, *2*, 301−306.

MA0488764